Ratiometric biosensors based on dimerization-dependent fluorescent protein exchange

Yidan Ding[1], Jiao Li[2], Jhon Ralph Enterina[1], Yi Shen[1], Issan Zhang[3], Paul H Tewson[4], Gary C H Mo[5], Jin Zhang[5], Anne Marie Quinn[4], Thomas E Hughes[4,6], Dusica Maysinger[3], Spencer C Alford[1,7], Yan Zhang[2] & Robert E Campbell[1]

We have developed a versatile new class of genetically encoded fluorescent biosensor based on reversible exchange of the heterodimeric partners of green and red dimerization-dependent fluorescent proteins. We demonstrate the use of this strategy to construct both intermolecular and intramolecular ratiometric biosensors for qualitative imaging of caspase activity, Ca^{2+} concentration dynamics and other second-messenger signaling activities.

Strategies for converting fluorescent proteins (FPs) into active biosensors of intracellular biochemistry are few in number and are technically challenging. The three most common methods are fluorescence resonance energy transfer (FRET) between two different hues of FP[1,2], bimolecular complementation of a split FP[3], and engineering of a single FP to respond to an analyte of interest[4,5]. Each method has distinct advantages and disadvantages that make it applicable to a particular range of biosensing applications that would be impractical with the other technologies. In an effort to expand the range of biosensor design strategies and applications, we recently introduced dimerization-dependent FP (ddFP) technology as a fourth option[6,7]. A ddFP is a pair of quenched or nonfluorescent FP-derived monomers that can associate to form a fluorescent heterodimer. One of the monomers (copy A) contains a chromophore that is quenched in the monomeric state. The second monomer (copy B) does not form a chromophore and acts only to substantially increase the fluorescence of copy A upon formation of the AB heterodimer. In the green and red fluorescent versions of ddFP, the A copies are referred to as GA and RA, respectively. We previously reported variants of B optimized to pair with either GA or RA, but we later discovered that the B variants can interchangeably complement both GA and RA (**Supplementary Fig. 1**).

The realization that GA and RA could compete for binding to the same B variant led us to conceive of the fluorescent protein exchange (FPX) biosensor design strategy (**Fig. 1a**). We reasoned that ratiometric fluorescent changes could be achieved through the exchange of one ddFP monomer between two complementary ddFP binding partners in response to a change in protein-protein interactions. Although either the A or the B copy could be exchanged (i.e., between two different B or A copies, respectively), B copy exchange is the preferred implementation because this would result in a ratiometric change from red to green (or vice versa) fluorescence.

To determine whether the FPX strategy was feasible, we constructed the gene encoding GA-DEVD-B, where DEVD represents the caspase-3 substrate sequence Asp-Glu-Val-Asp (ref. 2), and coexpressed it with RA in cultured mammalian cells (**Fig. 1b**). In this design, the green fluorescence should be initially bright owing to the linkage of GA to the B copy. Upon cleavage, the B copy would be free to exchange with the free RA protein, and the red fluorescence would increase as green fluorescence decreased. Indeed, cells stimulated to undergo apoptosis stochastically exhibited the expected change in fluorescence (**Fig. 1c** and **Supplementary Video 1**), with red-to-green ratio changes of approximately eightfold (**Fig. 1d**). Performing the same assay with RA-DEVD-B and GA gave similar results, albeit with opposite color changes (**Supplementary Fig. 2**). Owing to cell-to-cell variation in protein expression levels, and the differing affinities of GA and RA for the B copy (**Supplementary Fig. 1**), this assay is qualitative rather than quantitative.

To investigate whether FPX could be performed between two different cellular compartments, we performed imaging of apoptotic cells coexpressing ^{NES}RA-DEVD-B^{NLS} and GA^{NLS}, where NES represents a genetically fused nuclear export signal[8] and NLS represents a fused nuclear localization sequence[9] (**Fig. 1e**). Red fluorescence, initially dispersed through both the nucleus and cytoplasm, was lost upon activation of caspase-3 owing to liberation of B^{NLS} from RA. Translocation of B^{NLS} to the nucleus led to formation of a heterodimer with GA^{NLS} and an increase in green fluorescence (**Fig. 1f**,**g**, **Supplementary Fig. 3** and **Supplementary Video 2**). Analogous results were obtained with GA^{NES}-DEVD-B^{NLS} and RA^{NLS} (**Supplementary Fig. 4** and **Supplementary Video 3**). A compelling feature of the translocating FPX caspase biosensors is that the accumulation of the second color in the nucleus could be useful for long-term monitoring of low levels

[1]Department of Chemistry, University of Alberta, Edmonton, Alberta, Canada. [2]State Key Laboratory of Biomembrane and Membrane Biotechnology, College of Life Sciences, PKU (Peking University)-IDG (International Data Group)/McGovern Institute for Brain Research, Peking University, Beijing, China. [3]Department of Pharmacology and Therapeutics, McGill University, Montreal, Quebec, Canada. [4]Montana Molecular, Bozeman, Montana, USA. [5]Department of Pharmacology and Molecular Sciences, The Johns Hopkins University School of Medicine, Baltimore, Maryland, USA. [6]Department of Cell Biology and Neuroscience, Montana State University, Bozeman, Montana, USA. [7]Department of Bioengineering, Stanford University, Stanford, California, USA. Correspondence should be addressed to R.E.C. (robert.e.campbell@ualberta.ca).

RECEIVED 11 JULY 2014; ACCEPTED 28 OCTOBER 2014; PUBLISHED ONLINE 26 JANUARY 2015; DOI:10.1038/NMETH.3261

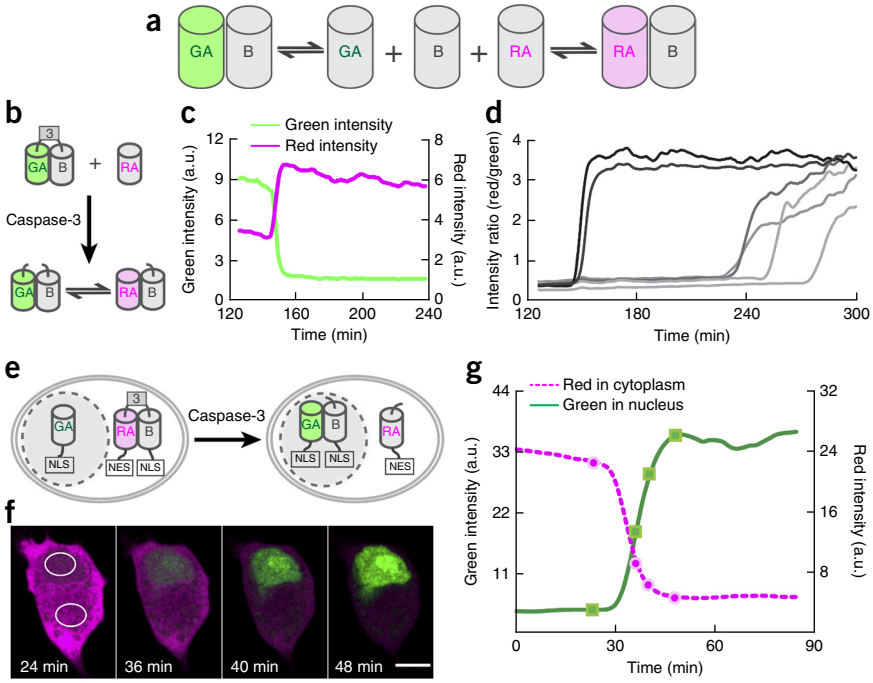

Figure 1 | The FPX strategy and application to imaging of protease activity. (**a**) Overview of the FPX strategy. (**b**) Green-to-red FPX detection of caspase-3 ('3' = DEVD substrate) activity. See **Supplementary Table 1** for construct details. (**c**) Green and red whole-cell intensities versus time for a single HeLa cell coexpressing GA-DEVD-B and RA and undergoing apoptosis. The *x* axis for all caspase activity imaging traces is time elapsed since 1 h after treatment with staurosporine. a.u., arbitrary units. (**d**) Whole-cell red-to-green intensity ratios versus time (average ratio change was 7.8-fold ± 0.9-fold (mean ± s.d.; $n = 6$ cells)). Each trace represents a single cell, treated and analyzed as in **c**. (**e**) A red-to-green FPX protease biosensor based on translocation of the dark B copy. (**f**) Selected merged frames (see **Supplementary Video 2**) from two-color imaging of a staurosporine-treated HeLa cell coexpressing ^{NES}RA-DEVD-B^{NLS} and GA^{NLS}. Red fluorescence is represented as magenta. Scale bar, 10 µm. The cell shown is representative of 12 imaged cells in 3 separate experiments. (**g**) Intensity versus time for the regions of interest circled in **f**.

of protease activity. To demonstrate this application, we used GA^{NES}-DEVD-B^{NLS} and RA^{NLS} to monitor caspase-3–dependent neuritic pruning in cultured rat hippocampal neurons depleted of nerve growth factor[10] (**Supplementary Figs. 5** and **6**). Having demonstrated that the B copy could be exchanged, we next demonstrated that an A copy could be exchanged between a B copy in the cytoplasm and a B copy in the nucleus (**Supplementary Figs. 7–9** and **Supplementary Videos 4–6**). Attempts to perform translocation of the A copy from the nucleus to cytoplasm were not successful (**Supplementary Fig. 10**).

To determine whether FPX technology could be used to image dynamic and reversible protein-protein interactions, we applied the technology to the Ca^{2+}-dependent interaction of calmodulin (CaM) and the Ca^{2+}-CaM interacting peptide M13 (**Fig. 2a**). Fluorescence imaging of HeLa cells transfected with genes encoding RA-CaM, M13-B and free GA revealed that histamine-stimulated Ca^{2+} oscillations were associated with increases in red fluorescence and decreases in green fluorescence (**Fig. 2b,c** and **Supplementary Video 7**).

To explore the utility of this approach for imaging of other signaling processes, we created biosensors for phosphatidylinositol 4,5-bisphosphate (PIP_2) hydrolysis, protein kinase A (PKA) activation and extracellular signal-regulated kinase (ERK) activity. To image PIP_2 hydrolysis, we coexpressed RA fused to a pleckstrin

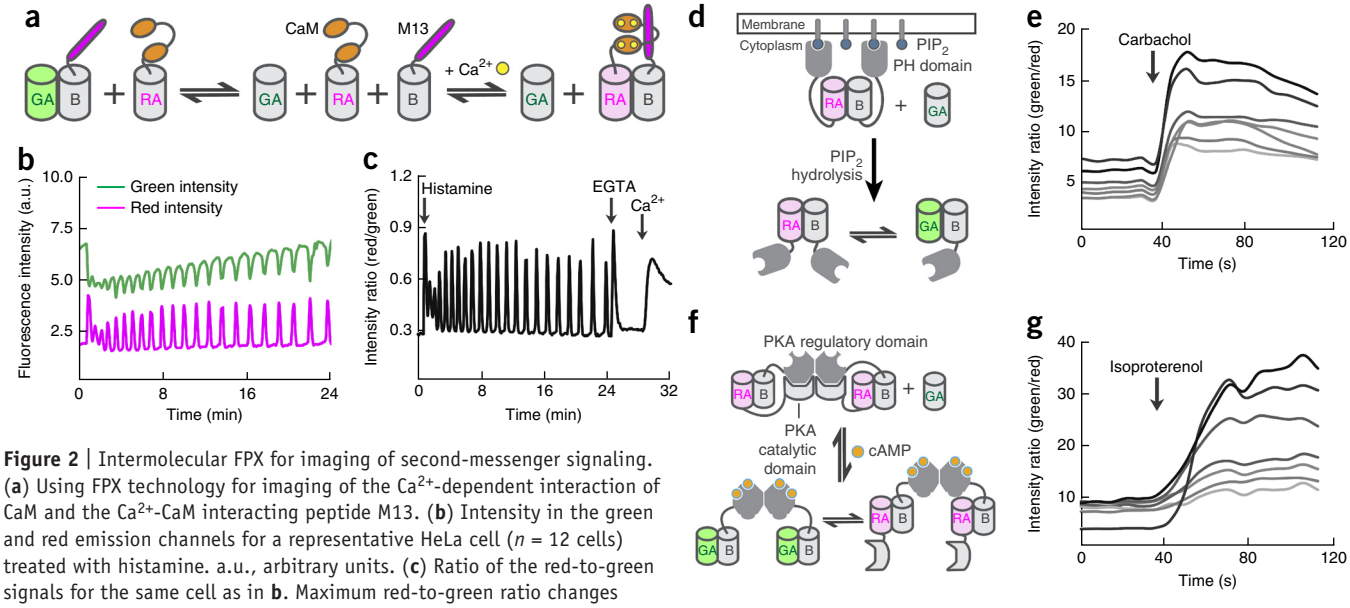

Figure 2 | Intermolecular FPX for imaging of second-messenger signaling. (**a**) Using FPX technology for imaging of the Ca^{2+}-dependent interaction of CaM and the Ca^{2+}-CaM interacting peptide M13. (**b**) Intensity in the green and red emission channels for a representative HeLa cell ($n = 12$ cells) treated with histamine. a.u., arbitrary units. (**c**) Ratio of the red-to-green signals for the same cell as in **b**. Maximum red-to-green ratio changes owing to histamine treatment was 3.2-fold ± 0.7-fold (mean ± s.d.; $n = 7$ cells). (**d**) FPX for imaging of PIP_2 hydrolysis to generate diacylglycerol and inositol 1,4,5-trisphosphate (IP_3). (**e**) Green-to-red ratio versus time for 7 cells expressing genes encoding the proteins represented in **d** and treated with carbachol. (**f**) FPX for imaging of cAMP-dependent PKA activation. (**g**) Green-to-red ratio versus time for 7 individual cells expressing genes encoding the proteins represented in **f** and treated with isoproterenol.

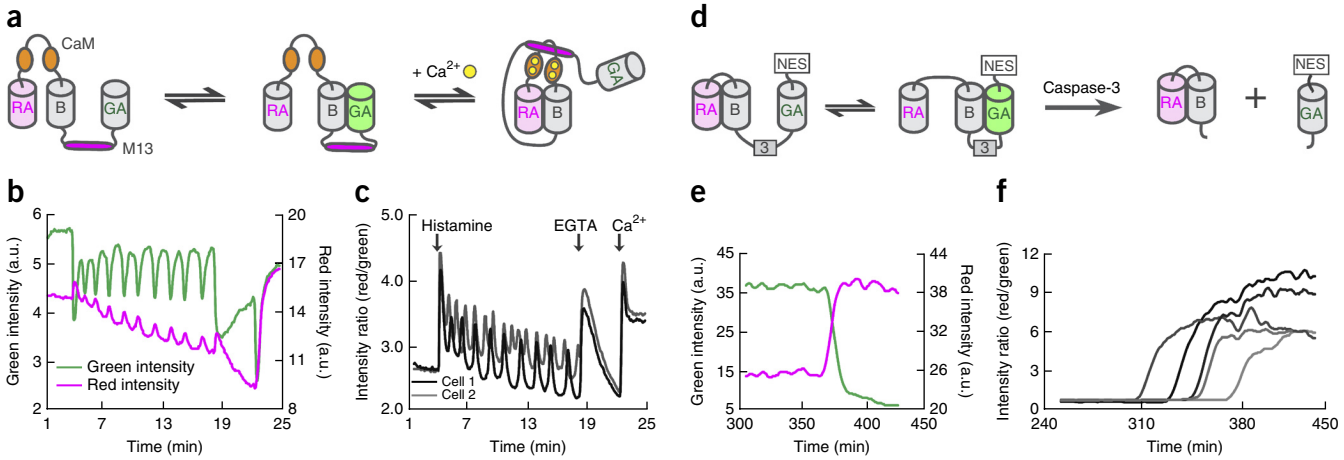

Figure 3 | Intramolecular FPX using tripartite single polypeptides. (**a**) Single-polypeptide FPX biosensor for Ca^{2+}. (**b**) Intensity versus time of green and red fluorescence for a representative HeLa cell (n = 18) expressing RA-CaM-B-M13-GA and undergoing histamine-induced Ca^{2+} oscillations. a.u., arbitrary units. (**c**) Red-to-green ratio versus time for the cell represented in **b** (cell 1) and a second cell (cell 2). (**d**) Single-polypeptide FPX for imaging of caspase-3 activity. (**e**) Whole-cell green and red intensities for a HeLa cell expressing RA-linker-B-DEVD-GA^{NES} and undergoing staurosporine-induced apoptosis. (**f**) Red-to-green intensity ratio versus time for multiple cells expressing the construct shown in **d**. The average red-to-green ratio change was 10-fold ± 5-fold (mean ± s.d.; n = 5 cells, each shown by a trace).

homology (PH) domain, B fused to a PH domain, and GA (**Fig. 2d**). Cells initially exhibited red fluorescence on the plasma membrane, which is consistent with a high effective concentration of RA and B subunits, and green fluorescence throughout the cytoplasm owing to an excess of the B-PH fusion. Stimulation with carbachol led to loss of red fluorescence on the membrane and a whole-cell increase in green-to-red ratio (**Fig. 2e**, **Supplementary Fig. 11a** and **Supplementary Video 8**). To image PKA activation, we coexpressed RA fused to the PKA catalytic domain, B fused to the PKA regulatory domain, and free cytosolic GA (**Fig. 2f**). Treatment with isoproterenol to stimulate elevation of cyclic AMP (cAMP) and dissociation of the catalytic and regulatory domains produced an increase in the green-to-red ratio (**Fig. 2g** and **Supplementary Fig. 11b**). To create an FPX-based biosensor of ERK activity, we replaced YPet and ECFP of the FRET-based EKAREV biosensor[11] with RA and B, respectively, and coexpressed this construct with GA^{NES}. Ratiometric responses comparable to those with EKAREV (~50%) were observed after treatment with epidermal growth factor (**Supplementary Fig. 12**).

We reasoned that it might be possible to combine all three components of the FPX system into a single polypeptide chain to simplify the transfection procedure while also substantially decreasing the high cell-to-cell variability in expression levels and fluorescence ratios associated with the intermolecular approach. To test this idea, we constructed a tripartite single-polypeptide Ca^{2+} biosensor with the structure RA-CaM-B-M13-GA (**Fig. 3a**). In this arrangement, we presume that the protein exists as an equilibrium mixture in which B is sometimes associated with RA and sometimes with GA. Although we could not predict in advance whether this equilibrium would favor the red or green state, we were confident that Ca^{2+}-dependent association of CaM and M13 would perturb the equilibrium. Indeed, we observed that the red-to-green ratio was initially ~3, and this increased to ~4 in response to histamine-induced Ca^{2+} oscillations (**Fig. 3b**,**c** and **Supplementary Video 9**). Photobleaching of the red state was more pronounced for the single-polypeptide Ca^{2+} biosensor than for the intermolecular Ca^{2+} biosensor (**Fig. 2a**–**c**). We reason that the intermolecular design benefits from exchange with the large pool of unbound RA (and GA) monomers that are in a dark, quenched state and thereby protected from photobleaching. Notably, for both the inter- and intramolecular FPX strategies, a useful ratiometric biosensor was created on the first attempt, supporting the idea that FPX is relatively insensitive to linker length and composition. In contrast, 28 designs were tested during the development of cameleon-1, the first FRET-based Ca^{2+} biosensor[12].

To determine whether single-polypeptide FPX constructs could also be applied to protease activity biosensing, we constructed RA-linker-B-DEVD-GA^{NES} (**Fig. 3d**). We expected this construct to initially exhibit a combination of green and red fluorescence due to intramolecular exchange of the B copy between the two A copies. Upon cleavage, GA would be released and RA would preferentially bind with B. Imaging of transfected cells undergoing apoptosis revealed a consistent baseline ratio and a pronounced increase in red-to-green ratio upon caspase cleavage (**Fig. 3e**,**f** and **Supplementary Video 10**). Analogous experiments for imaging of caspase-8 activity (RA-IETD-B-linker-GA^{NES}) with release of RA led to the expected increase in green-to-red ratio (**Supplementary Fig. 13** and **Supplementary Video 11**). To demonstrate the practical utility of this design, we constructed a caspase-1 biosensor (RA-linker-B-YVAD-GA) and used it as a marker of pro-inflammatory processes and pyroptotic cell death[13] in three cell lines exposed to inflammatory and non-inflammatory stimuli (**Supplementary Fig. 14**). A tripartite construct containing both caspase-8 and caspase-3 substrates (i.e., RA-IETD-B-DEVD-GA^{NES}) gave a decrease in green-to-red ratio during apoptosis (**Supplementary Fig. 15**). However, the very high caspase-3 activity (**Fig. 3f**) relative to caspase-8 activity (**Supplementary Fig. 13c**) complicated the interpretation of these results.

We have demonstrated the versatility of the FPX biosensing strategy by applying it in a variety of live-cell imaging applications. A limitation of FPX is that it is not suitable for quantitative imaging because of complications arising from variable protein expression levels (for intermolecular applications) and the inherent and differing affinities of GA and RA for the B copy.

In applications in which quantitation is not required, FPX minimizes the need for extensive biosensor optimization and provides a versatile new approach to building the next generation of biosensors.

METHODS

Methods and any associated references are available in the online version of the paper.

Accession codes. GenBank/EMBL/DDBJ, Addgene: KF976774, 50835; KF976776, 50840; KM979348, 60972; KM979349, 60973; KF976775, 50836; KF976777, 50842; KF976778, 50843; KF976779, 50849; KF976780, 50852; KP030819, 61017; KP030818, 36294; KP030820, 61018; KP030822, 61020; KP030821, 61019; KP030816, 36292; KP030817, 36293; KM891584, 60886; KM891581, 60883; KM891582, 60884; KM891585, 60887; KM891583, 60885; KP001564, 60936; KP001565, 60937; KM979350, 60974. See **Supplementary Table 1** for full details.

Note: Any Supplementary Information and Source Data files are available in the online version of the paper.

ACKNOWLEDGMENTS

We thank the University of Alberta Molecular Biology Service Unit, C.W. Cairo and R. Derda for technical assistance, and T. Meyer (Stanford) for the PLCδ-encoding gene. Funding support was provided by Canada Research Chairs (R.E.C.), the Alberta Glycomics Centre (R.E.C.), the Canadian Institutes of Health Research (NHG 99085 and MOP 123514 to R.E.C. and MOP 119425 to D.M.), the Natural Sciences and Engineering Research Council of Canada (Discovery grant to R.E.C. and a CGSD3 Scholarship to S.C.A.), Alberta Ingenuity PhD Scholarships (S.C.A. and Y.S.), a National Science Foundation of China Major Research Grant (91132718 to Y.Z.), the Beijing Natural Science Foundation (7142085 to Y.Z.), US National Institutes of Health DP1 CA174423 (to J.Z.) and 5R44NS082222 (to A.M.Q. and T.E.H.), and US National Science Foundation Small Business Innovation Research (SBIR) 1248138 and Montana SBIR matching funds #13-50 RCSBIR-003 (A.M.Q.).

AUTHOR CONTRIBUTIONS

Y.D., J.Z., P.H.T., A.M.Q., T.E.H., D.M., S.C.A., Y.Z. and R.E.C. conceived of and designed experiments. Y.D. assembled all constructs except for the PIP_2, PKA and ERK biosensors and performed imaging of all caspase-3, caspase-8 and caspase-9 biosensors and the three-polypeptide Ca^{2+} biosensor. J.L. performed imaging with the caspase-3 biosensor in neurons. J.R.E. determined heterodimer affinities *in vitro*. Y.S. performed imaging of the single-polypeptide Ca^{2+} biosensor. I.Z. performed imaging of the caspase-1 biosensor. P.H.T. assembled and performed imaging of the PIP_2 and PKA biosensors. G.C.H.M. assembled and performed imaging of the ERK biosensor. All authors were involved in data analysis, and Y.D., J.Z., T.E.H., D.M., S.C.A., Y.Z. and R.E.C. wrote the manuscript.

COMPETING FINANCIAL INTERESTS

The authors declare competing financial interests: details are available in the online version of the paper.

1. Miyawaki, A. *et al. Nature* **388**, 882–887 (1997).
2. Xu, X. *et al. Nucleic Acids Res.* **26**, 2034–2035 (1998).
3. Hu, C.D., Chinenov, Y. & Kerppola, T.K. *Mol. Cell* **9**, 789–798 (2002).
4. Nagai, T., Sawano, A., Park, E.S. & Miyawaki, A. *Proc. Natl. Acad. Sci. USA* **98**, 3197–3202 (2001).
5. Nakai, J., Ohkura, M. & Imoto, K. *Nat. Biotechnol.* **19**, 137–141 (2001).
6. Alford, S.C., Abdelfattah, A.S., Ding, Y. & Campbell, R.E. *Chem. Biol.* **19**, 353–360 (2012).
7. Alford, S.C., Ding, Y., Simmen, T. & Campbell, R.E. *ACS Synth. Biol.* **1**, 569–575 (2012).
8. Wen, W., Meinkotht, J.L., Tsien, R.Y. & Taylor, S.S. *Cell* **82**, 463–473 (1995).
9. Kalderon, D., Roberts, B.L., Richardson, W.D. & Smith, A.E. *Cell* **39**, 499–509 (1984).
10. Simon, D.J. *et al. J. Neurosci.* **32**, 17540–17553 (2012).
11. Komatsu, N. *et al. Mol. Biol. Cell* **22**, 4647–4656 (2011).
12. Miyawaki, A. & Tsien, R.Y. *Methods Enzymol.* **327**, 472–500 (2000).
13. Bergsbaken, T., Fink, S.L. & Cookson, B.T. *Nat. Rev. Microbiol.* **7**, 99–109 (2009).

ONLINE METHODS

General methods and materials. All synthetic DNA oligonucleotides were purchased from Integrated DNA Technologies. *Pfu* polymerase (Thermo Scientific) was used for standard PCR reactions. PCR products and products of restriction digests were purified by gel electrophoresis and extracted by GeneJET gel extraction kit (Thermo Scientific) according to the manufacturer's protocols. Restriction enzymes were purchased from New England BioLabs or Thermo Scientific. Site-directed mutagenesis was performed using Quikchange Lightning kit (Agilent), following the manufacturer's instruction. The cDNA sequences were confirmed by dye terminator cycle sequencing using the BigDye Terminator v3.1 Cycle Sequencing kit (Life Technologies). Sequencing reactions were analyzed at the University of Alberta Molecular Biology Service Unit. Cultured cells were not tested for the presence of *Mycoplasma*, as such contamination would not impact the conclusions made on the basis of our imaging results. The sequences of all primers are provided in **Supplementary Table 2**.

Protein purification and *in vitro* characterization. For expression and purification of A and B copy proteins, the genes were subcloned into pBAD/His B, and the resulting plasmids were used to transform ElectroMax DH10B *Escherichia coli* (Life Technologies). Single colonies were used to inoculate TB broth supplemented with 100 mg/L ampicillin. After 2 h, 0.02% L-arabinose was added to induce protein expression. Cultures were then further incubated at 30 °C for 15–20 h. Cells were harvested by centrifugation at 7,000 r.p.m. (relative centrifugal force (RCF) = 7,500*g* at maximum radius) for 10 min (Beckman), resuspended in Tris-Cl buffer (pH 7.4), and lysed using a high-pressure homogenizer (Constant System Ltd.) under 20,000 p.s.i. His-tagged soluble proteins were purified from cleared cell lysate by nickel-NTA resin (MCLAB). The lysate-resin mixture was transferred to a column and rinsed with wash buffer (50 mM Tris-HCl, 300 mM NaCl, 20 mM imidazole, pH 8.0). Proteins were then eluted from the resin using 50 mM Tris-Cl (pH 7.4) supplemented with 300 mM NaCl and 300 mM imidazole. Proteins were concentrated and buffer exchanged into Tris-Cl buffer (pH 7.4) using a centrifugal filter devices with a 10-kDa MWCO (EMD Millipore). Finally, a BCA assay and SDS-PAGE analysis were performed to determine protein concentration and confirm the purity.

For *in vitro* measurements of the dissociation constant (K_d) of various AB heterodimers, increasing amounts of the nonfluorescent B copy were added to a fixed amount of A copy, thereby generating a fluorescent AB complex. Fluorescence emission spectra were recorded using a QuantaMaster spectrofluorometer (Photon Technology International). Saturation binding curves were generated by plotting the integrated fluorescence emission intensity as a function of B copy concentration. Experimental data were fit using the Langmuir equation (Origin 9.0).

For *in vitro* measurements of caspase-3 activity in neurons, proteins were extracted in caspase lysis buffer (50 mM HEPES, pH 7.4, 0.1% 3-([3-cholamidopropyl]dimethylammonio)-1-propanesulfonate (CHAPS), 1 mM DTT, and 0.1 mM EDTA) for 10 min on ice followed by microcentrifugation to remove insoluble material. Protein concentration was determined by BCA assay (Pierce). Proteins (10 µg per 100 µL reaction assay) were added to 10 ng of recombinant active caspase (PharMingen) in assay buffer (20 mM PIPES, 30 mM NaCl, 10 mM DTT, 1 mM EDTA, 0.1% CHAPS, and 10% sucrose, pH 7.2) and 68.5 µM acetylated (Ac)-DEVD-7-amino-4-trifluoromethyl coumarin (AFC) for caspase-3. The caspase-3 activity was measured at 37 °C every 2 min for 1 h to determine the linear range of activity. On the basis of an AFC standard curve, the amount of released AFC was measured and the specific activity of the caspase-3 was determined as nanomoles of released AFC per microgram of protein per minute[14].

Assembly of reporter-gene plasmids. DNA encoding a nuclear exclusion sequence (NES; sequence LALKLAGLDIGS)[8] or a triplicate copy of a nuclear localization sequence (NLS; sequence DPKKKRKVDPKKKRKVDPKKKRKV)[9] was appended to either the 5′ or 3′ end of the gene of copy A or B to construct the fusions described in **Supplementary Table 1**. The gene sequences encoding A^{NES}, A^{NLS}, B^{NES}, or B^{NLS} were PCR amplified with primers containing a 5′ XhoI site and a 3′ KpnI site, or a set of primers containing a 3′ HindIII site and a 5′ KpnI site followed by a sequence encoding HSTHSHSSHTASHDEVDGA. The tandem heterodimer construct was built by ligating XhoI/KpnI digested fusions with KpnI/HindIII digested DEVD containing fusions into pcDNA3.1(+) (Life Technologies) with a three-part ligation. Tandem ddFP heterodimers for caspase-8 and caspase-9 biosensors were constructed in the same manner, except the DEVD sequence was replaced by IETD and LEHD sequence, respectively. To construct A^{NES}, A^{NLS}, B^{NES}, or B^{NLS}, the appropriate gene regions were amplified using primers encoding a 5′ XhoI site and a 3′ HindIII site. The XhoI/HindIII-digested fusions were then ligated into pcDNA3.1(+) cut with the same two enzymes. For the one-plasmid dual-caspase biosensor, RA-IETD-B-DEVD-GA^{NES}, two gene fragments and a HindIII- and XhoI-digested vector pcDNA3.1(+) were assembled in a three-part ligation. A previously created caspase-8 biosensor, containing a RA-B heterodimer with a duplicated IETD sequence as linker, was used as template for the first fragment. A 5′ primer containing a HindIII site and a 3′ primer containing a BamHI site were used to amplify the first fragment HindIII-RA-KpnI-2×IETD-B-BamHI. The second fragment was created by amplifying GA-NES using a 5′ primer containing a BamHI site and a sequence encoding the DEVD substrate sequence as well as a 3′ primer containing an XhoI site. The single plasmid caspase-3 biosensor, RA-linker-B-DEVD-GA^{NES}, was created by performing site-directed mutagenesis on RA-IETD-B-DEVD-GA^{NES} to replace the sequence encoding duplicated IETD with a linker sequence encoding an XhoI site. This additional site was used to facilitate rapid screening of ligation products by diagnostic analytical digestion. Similarly, the single-plasmid caspase-8 biosensor, RA-IETD-B-linker-GA^{NES}, was created by performing site-directed mutagenesis on RA-IETD-B-DEVD-GA^{NES} to replace the DEVD sequence with a linker encoding a KpnI site.

To construct the caspase-1 biosensor, RA-linker-B-YVAD-GA, we PCR-amplified GA using a 5′ primer containing BamHI site and sequence encoding three repeats of caspase-1 substrate YVAD as well as a 3′ primer containing a XhoI site. The BamHI/XhoI-digested PCR product was then ligated together with HindIII/BamHI-digested RA-linker-B-DEVD-GA^{NES} and HindIII/XhoI-digested pcDNA3.1(+). For caspase-1 activity imaging, plasmids were prepared in α-Select *E. coli* (Bioline) and isolated by Miniprep kit (Qiagen). DNA concentration was adjusted to 1 µg/µL in purified water, and plasmids were stored at −20 °C.

For the intermolecular Ca^{2+} biosensor, the previously reported RA-CaM and M13-B constructs were used[6]. GA^{NES} was prepared as described above. A three-part ligation was used to construct the gene encoding the intramolecular (single-plasmid) Ca^{2+} biosensor, RA-CaM-B-M13-GA^{NES}. The first fragment was amplified from template RA-CaM with primers containing a 5′ XhoI site and a 3′ BamHI site. The second fragment, B-M13-GA, was created by first replacing B in M13-B with GA, resulting in M13-GA. Subsequently, M13-GA was amplified with primers containing a 5′ EcoRI site and a 3′ HindIII site and then digested with EcoRI. A B copy was amplified with primers containing a 5′ BamHI and a 3′ EcoRI site and then digested with EcoRI. These two EcoRI-digested fragments were ligated and then digested with BamHI/HindIII, and the resulting fragment was used in a three-part ligation with the digested first fragment and XhoI/HindIII-digested pcDNA3.1(+).

To construct the PIP_2 biosensor, we ligated genes encoding RA and B to the 5′ end of the pleckstrin homology (PH) domain of PLCδ (amplified from Addgene plasmid 21262)[15]. The ligation product was inserted into a modified pcDNA3.1 using the In-Fusion Cloning kit (Clontech). To construct the cAMP-dependent PKA biosensor, we fused the gene encoding RA to the 5′ end of the catalytic subunit of PKA, and the gene encoding B was fused to the 3′ end of the regulatory subunit. Plasmids encoding the catalytic and regulatory subunits of PKA were obtained from OriGene (MC200197) and Source Bioscience (IRATp970F0898D), respectively. Ligation products were separately cloned into modified pcDNA3.1 with the In-Fusion Cloning kit (Clontech).

The gene construct for the ERK biosensor was assembled in a pcDNA3.0 vector with a modified multiple cloning site. The modified EKAREV[11] with RA and B was cloned via two steps. In the first step, the RA fragment containing a short linker flanked by a BglII/KpnI at its 3′ end was generated and ligated to a PCR-generated B fragment using the sites KpnI/EcoRI together in a linearized pRSET-B vector, forming a tandem RA-B construct. Replacing the short linker within the tandem construct with a PCR-generated fragment containing the EKAREV phosphorylation-responsive domain through the sites BglII/KpnI yielded the desired product. The constructs were then subcloned into linearized pcDNA3.0 via the BamHI/EcoRI sites.

Cell culture and transfection. HeLa cells used for caspase-3, caspase-8, caspase-9, and Ca^{2+} imaging experiments were maintained in Dulbecco's modified Eagle medium (DMEM) supplemented with 10% fetal bovine serum (FBS) and GlutaMAX (Life Technologies) at 37 °C and 5% CO_2. Transient transfections of pcDNA3.1(+) expression plasmids were performed using Turbofect (Thermo Scientific). HeLa cells in 35-mm imaging dishes were incubated with 1 mL of DMEM (FBS free) for 10 min and then transfected with 1 μg of plasmid DNA that had been mixed with 2 μL of Turbofect (Thermo Scientific) in 0.1 mL of DMEM (FBS free). The culture medium was changed back to DMEM with 10% FBS after 2 h incubation at 37 °C.

For imaging of caspase-3 activity in neurons, rat primary neurons were cultured from male and female newborn Sprague Dawley (SD) rat hippocampus following the regulations of Peking University Animal Care and Use Committee[16]. In brief, fresh rat hippocampal tissues were dissociated with 0.25% trypsin (Life Technologies), which was then inactivated by 10% decomplemented FBS (Thermo Scientific). The mixture was triturated through pipette to make a homogeneous mixture. After filtering the mixture through 70-μm sterilized filters, the flow-through was centrifuged. The pellet was then washed once by PBS and once by DMEM containing 0.225% sodium bicarbonate, 1 mM sodium pyruvate, 2 mM L-glutamine, 0.1% dextrose, 1× penicillin-streptomycin (Life Technologies) with 5% FBS. Cells were then plated on dishes coated with poly(L-lysine) (Sigma) or on glass coverslips at the density of 3×10^6 cells/mL. Neurons were incubated at 37 °C in DMEM without phenol red with 5% FBS and 5% CO_2. Cytarabine was added to culture medium 24 h after plating at 10 μM to inhibit cell growth. Medium was changed every 48 h. Thin-walled borosilicate glass capillaries (outer diameter = 1.0 mm, inner diameter = 0.5 mm) with microfilament (MTW100F-4, World Precision Instrument) were pulled with a Flaming/Brown Micropipette Puller (P-97, Sutter) to obtain injection needles with a tip diameter of ~0.5 μm. Microinjections were performed in the cytosol of each cell using the Eppendorf Microinjector FemtoJet and Eppendorf Micromanipulator. Neurons were injected with 25 fL/shot at an injection pressure of 100 hPa, a compensation pressure of 50 hPa, and an injection time of 0.1 s. GA^{NES}-DEVD-B^{NLS} and RA^{NLS} were injected into the cytosol at 30 ng/mL. Approximately 90% of neurons survived the injections for at least 16 d (ref. 17).

For imaging of PIP_2 and PKA activities, HEK293 cells were cultured in Eagle's minimal essential medium (EMEM, ATCC) supplemented with 10% FBS and penicillin-streptomycin (Life Technologies) at 37 °C in a 5% CO_2 atmosphere. Prior to cell seeding, 96-well glass-bottom plates were coated with poly(D-lysine) (Fisher Scientific). Cells were seeded and transfected using Lipofectamine 2000 (Life Technologies) according to the manufacturer's protocol and incubated for 30–48 h at 37 °C in 5% CO_2. For PIP_2 imaging, HEK293 cells were cotransfected with the DNA vector encoding the PIP_2 biosensor (50 ng), plus the vector encoding GA (50 ng), plus a vector (30 ng) encoding human M1 muscarinic acetylcholine receptor (M1 mAChR). For PKA imaging, cells were transfected with the vector encoding the PKA biosensor (50 ng), plus the vector encoding GA (50 ng), and a vector (30 ng) encoding the rat beta-adrenergic receptor (β-AR). Vectors encoding M1 mAChR and β-AR were obtained from the Missouri S&T cDNA Resource Center (http://www.cdna.org/).

For imaging of ERK activity, HEK293 cells were maintained in DMEM growth medium supplemented with 10% FBS, 1% penicillin and streptomycin. All cells were transfected at an approximate confluency of 70% using Lipofectamine 2000 reagent and incubated for 24 h before imaging. All cells were imaged in Hank's balanced salt solution (HBSS) buffer at room temperature.

For caspase-1 activity imaging, the MCF-7, U251, and HepG2 cell lines were obtained from the ATCC. Unless otherwise specified, MCF-7 and U251 cells were cultured in DMEM and HepG2 cells were cultured in minimum essential medium (MEM) containing 10% FBS, 2 mM L-glutamine, 100 IU/mL penicillin, 100 μg/mL streptomycin (Life Technologies), and 1% non-essential amino acids. Cells were incubated at 37 °C with 5% CO_2. Cells were seeded in black 96-well plates (Corning) at a density of 10,000 cells per well and cultured for 24 h. Transfection was conducted in the absence of antibiotics, using Lipofectamine 2000 (Life Technologies), following the procedure recommended by the manufacturer. The transfection complexes were kept for 12 h,

doi:10.1038/nmeth.3261

after which the medium was refreshed, and cells were allowed to recover for another 12 h before treatment.

Cell treatments and imaging conditions. Transfected HeLa cells were imaged using an Axiovert 200M (Zeiss), a laser scanning confocal LSM-700 (Zeiss), or a Nikon Eclipse Ti. The Axiovert 200M was equipped with a 75-W xenon-arc lamp, a 40× objective lens (numerical aperture (NA) = 1.3; oil), and a 14-bit CoolSnap HQ2 cooled charge-coupled device (CCD) camera (Photometrics) and was driven by open-source μManager software. The LSM-700 (Zeiss) was equipped with 10-mW 488-nm and 555-nm solid-state laser, 63× objective lens (NA = 1.40; oil), two high-sensitivity, and low-noise adjustable PMTs and was driven by Zeiss's Zen software. The Nikon Eclipse Ti microscope was equipped with a 150-W Lumen 200 metal halide lamp (Prior Scientific), a 16-bit 512SC QuantEM CCD (Photometrics), a 25% neutral-density filter, and a 40× objective (NA = 0.95; air) and was driven by a NIS-Elements AR 3.0 software package (Nikon).

For imaging of caspase-3, caspase-8, and caspase-9 activities in HeLa cells, apoptosis was initiated by treatment with 2 μM staurosporine at 24–48 h post-transfection. Cells were maintained in HEPES-buffered HBSS (HHBSS) and subjected to imaging at 1- or 2-min intervals for 4–6 h. For imaging of Ca^{2+} concentration dynamics in HeLa cells, transfected cells were imaged in HHBSS and were consecutively treated with histamine (0.1 mM) in Ca^{2+}-free HHBSS, EGTA (10 mM) in Ca^{2+}-free HHBSS with ionomycin (5 μM), and $CaCl_2$ (10 mM) in HHBSS with ionomycin (5 μM). Images were acquired at 5-s or 10-s intervals for up to 60 min, using an inverted Nikon Eclipse Ti microscope as described above. All cell images were processed and analyzed using ImageJ (http://imagej.nih.gov/ij/). All intensity and ratio traces were plotted as scatter charts with smoothed lines in Microsoft Excel.

For imaging of the PIP_2 biosensor and the cAMP biosensor, EMEM was replaced with 1× Dulbecco's phosphate-buffered saline (DPBS) before live-cell imaging. A Zeiss Axiovert S100TV inverted microscope equipped with computer-controlled excitation and emission filter wheels, shutters, and a Qimaging Retiga Exi CCD camera was used to image cells at 25 °C using the 10× objective lens (NA = 0.3). Red fluorescence was detected with 572/20-nm excitation and 630/30-nm emission filters. Green fluorescence was detected with 480/20-nm excitation and 535/25-nm emission filters. To analyze the image stacks, we defined background fluorescence as a region of the image that contained no cells. The average value of the background region was subtracted frame by frame from measurements of the mean pixel values from cells. Red and green fluorescence was measured before and after addition of an agonist to activate the coexpressed receptor. PIP_2 activation was done by the addition of 50 μM carbachol (Sigma). PKA activation was done by the addition of 50 μM isoproterenol (Sigma).

For imaging of caspase-3 activity during neuritic pruning, cell treatments for experiments were performed after 7 d in culture. Nuclear fluorescence intensity of live cells was measured with ImageJ by limiting the region of interest (ROI) to the area defined by Hoechst nuclear staining. Staurosporine (Sigma) was added to the culture medium to a final concentration of 5 μM. After a 6-h treatment, the neurons were subject to imaging for 2 h. NGF-free medium with 1:20,000 dilution of anti-NGF neutralizing antibody (Alomone Labs, ALM-006) was added to the neurons for 24 h before the images were taken. The nuclei were costained by Hoechst 33342 (1 μg/mL, Sigma). The nuclear fragmentation was analyzed with a fluorescence live-cell imaging microscope (Olympus) by counting the number of fragmented nucleus out of a total of 100 nuclei in each treatment group.

Epifluorescence imaging of ERK activity was performed on a Zeiss Axiovert 200M microscope equipped with a xenon arc lamp and a cooled CCD, under a 40× oil-immersion objective. Ratiometric fluorescence imaging of FPX biosensors was performed using a 480/30-nm excitation filter and a 535/45-nm emission filter for green fluorescence and a 568/55-nm excitation filter and 653/95-nm emission filter for red fluorescence. All epifluorescence experiments were subsequently analyzed using the MetaFluor software (Molecular Devices).

For caspase-1 activity imaging, culture medium was refreshed before treatment. *E. coli* lipopolysaccharide (1 μg/mL; LPS; Sigma-Aldrich), adenosine triphosphate (5 mM; ATP; Sigma-Aldrich), tumor necrosis factor alpha (10 ng/mL; TNF-α; Sigma-Aldrich), palmitic acid (100 μM; Sigma-Aldrich), and ethanol (50 mM; Fisher) stocks were prepared in purified water. Staurosporine (0.5 μM; STS) and curcumin (10 μM; CUR; Sigma-Aldrich) were diluted in dimethylsulfoxide (DMSO). DMSO in-well concentration was kept below 0.1%. Treatment was maintained for 4 h in complete medium, after which cells were imaged using fluorescence microscopy. An automated platform (Operetta High Content Imaging System; PerkinElmer) was used to image cells displaying green (EGFP) and red (Alexa 594) signals. Caspase-1 activity was quantified as the whole-cell ratio of red-to-green fluorescence. Eleven fields were analyzed per well, with six wells per condition. Nontransfected cells were used as negative controls, in the presence or absence of drugs.

Statistical analysis. For analysis of caspase-3 activity in neurons, statistical significance was assessed by one-way analysis of variances (ANOVA). Sheffé's test was applied as a *post hoc* for the significant difference showed by ANOVAs. A P value of less than 0.05 was used as an indicative of statistical significance. Power analysis for each experiment to validate group size was done by SPSS V13.0.

For caspase-1 activity imaging, at least three independent experiments were performed for each condition, with six repeats per condition. All caspase-1 data are expressed as mean ± s.e.m. The Student's t-test with Bonferroni correction was used to analyze significant differences between group means (P values < 0.01 were considered to be significant).

14. Zhang, Y., Tounekti, O., Akerman, B., Goodyer, C.G. & LeBlanc, A. *J. Neurosci.* **21**, RC176 (2001).
15. Botelho, R.J. *et al. J. Cell Biol.* **151**, 1353–1368 (2000).
16. Cui, J. *et al. J. Neurosci.* **31**, 16227–16240 (2011).
17. LeBlanc, A. *J. Neurosci.* **15**, 7837–7846 (1995).